



ELSEVIER

Contents lists available at ScienceDirect

Biosensors and Bioelectronics

journal homepage: www.elsevier.com/locate/bios

Short communication

A sensitive and reliable dopamine biosensor was developed based on the Au@carbon dots–chitosan composite film

Qitong Huang^a, Hanqiang Zhang^a, Shirong Hu^{a,b,*}, Feiming Li^a, Wen Weng^{a,b}, Jianhua Chen^a, Qingxiang Wang^{a,b}, Yasan He^a, Wuxiang Zhang^a, Xiuxiu Bao^a^a Department of Chemistry and Environment Science, Minnan Normal University, Zhangzhou 363000, PR China^b Fujian Province University Key Laboratory of Analytical Science, Minnan Normal University, Zhangzhou 363000, PR China

ARTICLE INFO

Article history:

Received 26 July 2013

Accepted 2 September 2013

Available online 11 September 2013

Keywords:

Au nanoparticle

Carbon dots

Chitosan

Dopamine

Biosensor

Electrochemistry

ABSTRACT

A novel composite film of Au@carbon dots (Au@CDs)–chitosan (CS) modified glassy carbon electrode (Au@CDs–CS/GCE) was prepared in a simple manner and applied in the sensitive and reliable determination of dopamine (DA). The CDs had carboxyl groups with negative charge, which not only gave it have good stability but also enabled interaction with amine functional groups in DA through electrostatic interaction to multiply recognize DA with high specificity, and the Au nanoparticle could make the surface of the electrode more conductive. Compared with the bare GCE, CS/GCE, and CDs–CS/GCE electrodes, the Au@CDs–CS/GCE had higher catalytic activity toward the oxidation of DA. Furthermore, Au@CDs–CS/GCE exhibited good ability to suppress the background current from large excess ascorbic acid (AA) and uric acid (UA). Under the optimal conditions, selective detection of DA in a linear concentration range of 0.01–100.0 μM was obtained with the limit of 0.001 μM (3S/N). At the same time, the Au@CDs–CS/GCE was also applied to the detection of DA content in DA's injection with satisfactory results, and the biosensor could keep its activity for at least 2 weeks.

© 2013 Elsevier B.V. All rights reserved.

1. Introduction

Acting as one of the excitatory neurotransmitters, dopamine (DA) plays an important role in several physiological events such as behavior, mood, and movement. It is also involved in some diseases and in drug addiction. In addition, DA is available for intravenous medication, which acts on the sympathetic nervous system, to produce effects such as increasing heart rates and blood pressure (Ji et al., 2012; Suzuki et al., 2013; Wightman, 2006; Sulzer, 2011; Goldberg, 1972). Hence, determination of DA in vivo/vitro becomes increasingly important in clinical medical practice. Tremendous efforts have been made over the last 30 years to detect it, such as high performance liquid chromatography (Muzzi et al., 2008; Carrera et al., 2007), ultraviolet–visible spectrophotometry (Barreto et al., 2008), capillary electrophoresis (Thabano et al., 2009; Li et al., 2010), liquid chromatography–electrospray tandem mass spectrometry (El-Beqqali et al., 2007), fluorescence spectrometry (Khattar and Mathur, 2013; Chen et al., 2011), etc. Compared with other described methods, the direct electrochemical method for DA analysis, as a simple, rapid, and sensitive

alternative, is drawing increasing attention. However, on the bare glassy carbon electrode (GCE) the coexisting compounds such as uric acid (UA) or ascorbic acid (AA) in the biological samples can cause great interference due to the similar oxidation potential close to that of DA (Liu et al., 2013; Zhang et al., 2005). In addition, the accumulation of the oxidation product of AA or UA on electrode surface may lead to the electrode fouling with poor selectivity and reproducibility (Gonon et al., 1980). To resolve this problem, various materials have been employed to elaborate the surface of working electrodes or as the electrode materials, including boron-doped carbon nanotubes (Deng et al., 2009), graphene (Kim et al., 2010), gold nanoparticle (Raj et al., 2003), single wall carbon nanotubes (Habibi et al., 2011), Cu₂O/graphene (Zhang et al., 2011), Au nanoparticle–polyaniline nanocomposite layers (Stoyanova et al., 2011), multiwall carbon nanotubes (Allothman et al., 2010), hollow nitrogen-doped carbon microspheres (Xiao et al., 2011), and so on. Although most of these systems contributed to the detection of dopamine, these modified materials had either limitations with aspect to sensitivity or the material synthesis was sophisticated and expensive. Consequently, it is highly desirable to develop a sensor that is not only sensitive, selective and reliable but also simple, practical and economical in biological, pharmacological and toxicological fields.

For biosensing electrodes, Au nanoparticle is an excellent choice due to its conductivity, stability, biocompatibility and large

* Corresponding author at: Department of Chemistry and Environment Science, Minnan Normal University, Zhangzhou 363000, PR China.
Tel./fax: +86 596 2528075.

E-mail address: Hushirong6666@163.com (S. Hu).

surface area (Hsu et al., 2012). Carbon dots (CDs) as a class of 'zero-dimensional' carbon nanomaterials have recently received considerable attention because of their advantageous characteristics. Compared with conventional semiconductor quantum dots, CDs are superior in terms of low cytotoxicity, excellent biocompatibility, simple synthesis, economy and remarkable conductivity (Liu et al., 2012; Dai et al., 2012; Chen et al., 2013). The CDs can provide abundant carboxyl groups at the surface which can significantly enhance the redox response of dopamine. In this paper, we reported the synthesis of Au@carbon dots (Au@CDs), and the Au@CDs nanostructures could be used as electrochemical labels with signal amplification technique as the CDs could increase surface area of the electrode and Au nanoparticle could make the surface of the electrode more conductive. Then a novel composite film of Au@CDs–chitosan (CS) modified GCE (Au@CDs–CS/GCE) was prepared, and introduced it into a sensor for the rapid, simple and sensitive determination of DA. Under the optimal conditions good linearity was observed between the differential pulse voltammetric peak current and the concentration of DA in the range from 0.01 μM to 100 μM in a pH 7.0 phosphate buffer solution. Meanwhile, the Au@CDs–CS/GCE was applied to the detection of DA content in injection solution.

2. Experimental

2.1. Reagents and instrumentation

Sucrose, chitosan, chloroauric acid and dopamine were obtained from Sinopharm Chemical Reagent Co., Ltd. (Shanghai, China). Oil acid, glacial acetic acid, ascorbic acid, citric acid and polyethylene glycol-200 were purchased from Xilong Chemical Co., Ltd. (Guangdong, China). Phosphate buffer solution was from Shanghai Kangyi Instrument Co., Ltd. (Shanghai, China). All other reagents are analytical reagents. Nanopure deionized and distilled water (18.2 M Ω) was used throughout all experiments.

Electrochemical experiments such as cyclic voltammetry (CV) and differential pulse voltammetry (DPV) were carried out on a CHI 650D electrochemical workstation (Shanghai ChenHua Instruments Co., China). A conventional three-electrode system was used for all electrochemical experiments, which consisted of a platinum wire as auxiliary electrode, an Ag/AgCl/saturated KCl as reference electrode, and a bare or modified GCE as working electrode. The pH measurements were carried out on a PHS-3C exact digital pH metre (Shanghai Mettler-Toledo Instruments Co., Ltd.), which was calibrated with standard pH buffer solutions. The UV–vis absorption was registered by a mapada UV-1800PC (Shanghai China). The surface morphology of the Au@CDs–CS film was observed with atomic force microscopy (AFM, CSPM5500, China). Transmission electron microscope (TEM) was performed on a JEM-1230 electron microscope (JEOL, Ltd., Japan) at 300 kV. All experiments were conducted at room temperature.

2.2. Synthesis of CDs, Au nanoparticle and Au@CDs

According to Chen's method (Chen et al., 2013), 10 g sucrose and 20 ml oil acid were put into a three neck flask at 215 °C for 5 min under vigorous magnetic stirring and nitrogen protection to yield CDs. The sucrose slowly melted at 180 °C and turned from an orange suspension to a clear brownish solution. After cooling, the supernatant liquid was discarded and the solid brownish product was obtained at the bottom of flask. The precipitate was dissolved with 40 ml water, and then it was extracted with hexane several times in order to remove remaining oil acid. At last, the CDs were dialyzed for 24 h with the dialysis membranes of 1000 cutoffs, diluted to 500.00 mL with water and then stored at 4 °C for use.

Au nanoparticle was prepared according to the literature (Frens, 1973): 25 mL of HAuCl₄ (0.01% by weight) was heated to boiling; then, 375 mL aqueous solution of sodium citrate (1% by weight) was added. After reaction for 30 min, a wine red suspension of Au nanoparticle was obtained.

The synthesis of Au@CDs is as follows: 100 μL aqueous solution of HAuCl₄ (1.0 mg mL⁻¹) was added to 100 μL CDs solution (8.0 mg mL⁻¹). The mixed solution was kept at 100 °C for 80 min to yield a stable purple solution of Au@CDs (Luo et al., 2012). Scheme S1 (see Scheme S1 in the Supplementary materials) shows the synthesis of CDs and Au@CDs.

2.3. Electrode preparation

The GCE was polished to a mirror-like surface with 1.0 μm , 0.3 μm , and 0.05 μm α -alumina slurry then washed successively with distilled water, ethanol and distilled water in an ultrasonic bath, and dried in air before use.

Synthesis of Au@CDs–CS composite film: 100 μL 1.0% CS solution was added to 200 μL Au@CDs solution with vigorous ultrasonication. Then with a microinjector, 5.0 μL of the mixture solution was cast on the surface of GCE, and left to dry in an oven at 60 °C for 30 min.

3. Results and discussion

3.1. Characterization of CDs, Au@CDs and CDs–CS/GCE

The morphology of CDs (see Fig. S1A in the Supplementary materials) and Au@CDs (see Fig. S1B in the Supplementary materials) was characterized by TEM; typical UV–vis absorption spectra of CDs (a), Au (b) and Au@CDs (c) was shown in Fig. S1C (see Fig. S1C in the Supplementary materials). The Au@CDs had strong absorption bands at 282 nm and 536 nm. These values are consistent with previous reports (Chen et al., 2013; Luo et al., 2012).

AFM images of bare GCE and Au@CDs–CS/GCE film are shown in Fig. S2 (see Fig. S2 in the Supplementary materials). They show that the bare GCE surface is relatively smooth with the average roughness of 1.13 nm (see Fig. S2A in the Supplementary materials) whereas the average roughness of GCE is 117 nm after being modified by Au@CDs–CS (see Fig. S2B in the Supplementary materials), and irregular round islands appeared, which explains how the surface morphology changed the roughness. This result demonstrated that Au@CDs–CS film was deposited on the GCE surface.

3.2. Cyclic voltammetric behavior of DA on the Au@CDs–CS/GCE

The electrochemical responses of DA at GCE, CS/GCE, CDs–CS/GCE and Au@CDs–CS/GCE were examined using CV in 0.2 mM DA solution. As shown in Fig. 1, at a bare GCE (a), a pair of redox peaks appeared. After casting CS on the GCE (b), the redox peaks disappeared and the CDs–CS (c) or Au–CS (d) was fixed on the GCE surface, the redox peaks increased a little. However, for Au@CDs–CS modified GCE (e), the redox peaks increased considerably, which was due to the unique properties of Au@CDs and CS; the CS backbone together with Au@CDs introduced obviously sensitized the electrochemical redox of DA. Hence, this electrochemical platform based on CS and Au@CDs offered enhanced determination sensitivity for DA. A possible reaction mechanism of Au@CDs–CS/GCE with DA is discussed, which is shown in Scheme S2 (see Scheme S2 in the Supplementary materials). The CS is a biological cationic macromolecule with primary amines, and there are diols, amine functional groups, and phenyl in the DA

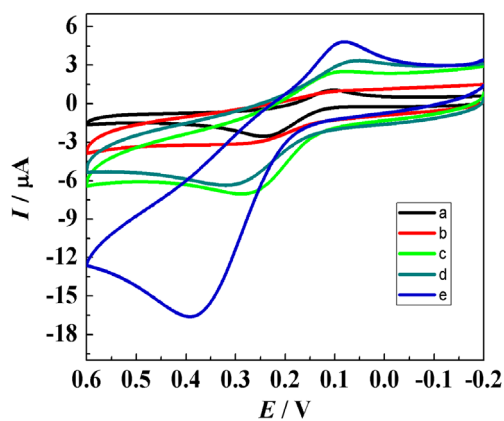


Fig. 1. CV of 0.20 mM DA recorded on bare GCE (a), CS/GCE (b), CDs-CS/GCE (c), Au-CS/GCE (d) and Au@CDs-CS/GCE (e) in the pH 7.0 phosphate buffer solution.

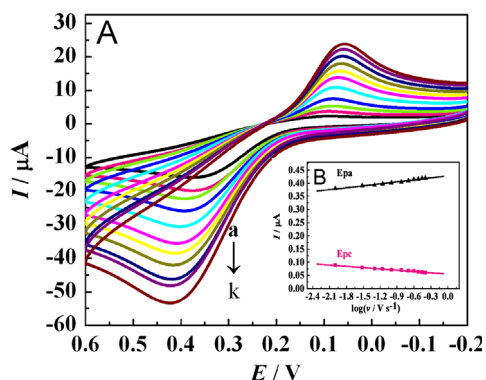


Fig. 2. (A) CV of 0.25 mM DA on Au@CDs-CS/GCE in the pH 7.0 phosphate buffer solution at various scan rates (a–k: 0.01, 0.03, 0.05, 0.07, 0.1, 0.15, 0.20, 0.25, 0.30, 0.35, 0.40 V s⁻¹). (B) The relationships of E_{pa} (a) and E_{pc} (b) with $\log v$.

molecules; therefore, it makes the system have a higher degree of irreversibility. However, the CS could make the Au@CDs to be on electrode membrane easily and it could avoid the interference of AA and UA (Fernandes et al., 2010; Ge et al., 2009) in the phosphate buffer solution of pH=7.0. Meanwhile, the CDs had carboxyl groups with negative charge, which not only gave it good stability but also enabled interaction with amine functional groups in DA through electrostatic interaction to multiply recognize DA with high specificity; the Au nanoparticle could also increase the current as it could make the surface of the electrode more conductive.

3.3. Effects of scan rate

The effect of scan rate on the redox of DA was also investigated. Fig. 2A reveals the CV of 0.200 mM DA at Au@CDs-CS/GCE with different scan rates. The redox peaks current increased gradually with the increase of scan rate. As shown in Fig. 2A, the redox peak current of DA increased linearly with the square root of scan rate in the range of 0.01–0.4 V s⁻¹, which indicated that the electroredox of DA on Au@CDs-CS/GCE is a typical diffusion controlled process. Moreover, with the increased scan rate, the redox potential of DA shifted positively. The relationship between the potential and scan rate could be described through the following equations by Laviron (Laviron, 1979):

$$E_{pa} = E^{0'} + \frac{2.3RT}{(1-\alpha)nF} \log \nu \quad (1)$$

$$E_{pc} = E^{0'} - \frac{2.3RT}{\alpha nF} \log \nu \quad (2)$$

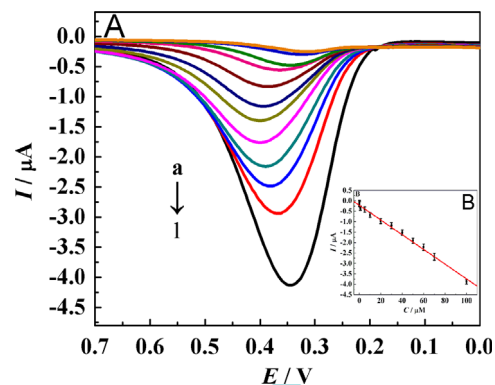


Fig. 3. (A) DPV of DA with increasing concentration (from a to l: 0.01, 1.0, 5.0, 10.0, 20.0, 30.0, 40.0, 50.0, 60.0, 70.0, 100.0 μM). (B) The relationship of the I_{pa} with the concentration of DA.

$$\log k_s = \alpha \log(1-\alpha) + (1-\alpha) \log \alpha - \log \frac{RT}{nFv} - \frac{(1-\alpha)\alpha nF \Delta E_p}{2.3RT} \quad (3)$$

where α is the electron transfer coefficient, n is the number of transfer electrons, k_s is the standard heterogeneous rate constant, R , T and F have their usual significance, E_{pa} is the oxidation peak potential and E_{pc} is the reduction peak potential. Generally, in the electrochemical reaction, the value of α , n can be easily calculated from the slope of $E_{pa}-\log \nu$ and $E_{pc}-\log \nu$ with the linear regression equations were E_{pa} (V) = 0.0966 $\log \nu$ (V s⁻¹) + 0.389 ($R=0.995$) and E_{pc} (V) = -0.0637 $\log \nu$ (V s⁻¹) + 0.0806 ($R=0.993$), which is shown in Fig. 2B. After computations $\alpha=0.40$, $n=1.82$, $k_s=0.22$ s⁻¹, which illustrating that the electrochemical oxidation of DA at the Au@CDs-CS/GCE is a diffusion-controlled process and not a surface-controlled process (Prasad et al., 2013; Qian et al., 2013).

3.4. pH effect

The effect of buffer pH on the current response of 0.5 mM phosphate buffer solution and 0.3 mM DA solution on Au@CDs-CS/GCE was investigated in the pH range from 5.0 to 9.0 by CV; the result is shown in Fig. S3 (see Fig. S3 in the Supplementary materials). The oxidation peak potential shifted negatively with the increase of pH value, indicating that protons are involved in the electrode reaction. A good linear relationship between E_{pa} and pH was constructed with linear regression equation as E_{pa} (V) = -0.0612 pH + 0.833 ($R=-0.992$). The slope value of -61.2 mV/pH shows that the electron transfer was accompanied by an equal number of protons, which is consistent with that reported in literatures (Raj and Osaka, 2001). At the same time, when the pH value increased from 5.0 to 7.0, the anodic peak current of DA increased. Nevertheless, when the pH was beyond 7.0, the peak current conversely decreased. This phenomenon was probably due to the dissociation of the phenolic moiety to produce the corresponding anion. Therefore, considering the sensitive determination for DA, the phosphate buffer solution of pH=7.0 was chosen for the subsequent analytical experiments.

3.5. Interference effect

As known, using a bare GCE, the oxidation peak potentials for ascorbic acid (AA), uric acid (UA) and DA are very close to each other and thus it is difficult to separate these compounds due to their overlapping signals (Zhang et al., 2005a). This problem can be eliminated by electrostatic attraction; since the Au@CDs-CS film is in its anionic form at the working electrode surface in the pH 7.0 phosphate buffer solution, both AA (pKa=4.1) and UA (pKa=5.75) are negatively charged, but DA (pKa=8.89) is positively

charged at physiological pH=7.0 (Wang et al., 2009b). So, Au@CDs-CS, as a cationic exchanger at the GCE surface, selectively attracts cationic DA and allows it to pass through to the electrode surface. Additionally, the CDs had carboxyl groups with negative charge, which could prevent anionic AA and UA from reaching the electrode surface. As a result, AA and UA did not exchange electrons with the electrode. As shown in Fig. S4 (see Fig. S4 in the supplementary materials), it could be concluded that the presence of AA (A) and UA (B) did not interfere in the DA determination.

In addition, other influences from common co-existing substances were also investigated. When the relative error (Er) exceeded 5%, each substance was considered as an interfering agent. It was found that most ions and common substances at high concentration caused only negligible change: Na⁺, K⁺, Cl⁻, NO₃⁻, SO₄²⁻ (> 500 fold), Ca²⁺, Zn²⁺, Mg²⁺, (150 fold), lysine, cysteine, glucose, citric acid and aspartic acid (100 fold). The results indicated that the Au@CDs-CS/GCE exhibited good selectivity for DA detection.

3.6. Calibration plot and limit of detection

By using the more sensitive differential pulse voltammetry (DPV) as the detection method, the Au@CDs-CS/GCE was further used for the DA detection. Under the optimal conditions, the oxidation peak current (I_{pa}) of DA increased with its concentration in the range from 0.1 μM to 30 μM with typical DPV shown in Fig. 3, with the linear regression equations as I_{pa} (μA) = -0.0353C (μM) - 0.212 ($R=0.997$). The detection limit was calculated as 1.0 nM, which is lower than those of some previous reports (see Table S1 in the Supplementary materials), which illustrates that Au@CDs-CS/GCE has good sensitivity and wide linear range. The electrode was put into a vacuum drying oven at 25 °C, and DA samples were determined every 48 h. Fig. S5 (see Fig. S5 in the Supplementary materials) shows that the electrode had a wonderful stability after 2 weeks.

3.7. Application of the probe

In order to evaluate the applicability of the proposed method to the determination of DA in pharmaceutical preparations, we examined this ability in differential pulse voltammetric determination of DA concentration in an injection solution based on the repeated differential pulse voltammetric responses ($n=5$) of the diluted analytes and the samples that were spiked with specified concentration of DA, and using the standard addition method, measurements were made of DA concentrations in the pharmaceutical preparations and of the recovery rate of the spiked samples. The results are listed in Table S2 (see Table S2 in the Supplementary materials).

4. Conclusions

In this study, we developed and characterized a new DA sensor based on the Au@CDs-CS/GCE electrode with high sensitivity, nice specificity and good stability. Under the optimal conditions, selective detection of DA in a linear concentration range of 0.01–100.0 μM was obtained with the limit of 0.001 μM (3S/N). Furthermore, Au@CDs-CS/GCE electrode exhibited good ability to suppress the background current from large excess AA and UA. Meanwhile, the Au@CDs-CS/GCE was applied also to the detection of DA content in DA's injection with satisfactory results, and the biosensor could keep its activity for at least two weeks. Therefore, Au@CDs-CS/GCE electrode is a promising analytical platform for detecting dopamine.

Acknowledgments

This project was supported by the Science and Technology Foundation of the National General Administration of Quality Supervision in China (2012QK053), the Fujian Province Natural Science Foundation (2012D136), and the Minnan Normal University Graduate Students' Scientific Research Projects (No. 1300-1314).

Appendix A. Supporting information

Supplementary data associated with this article can be found in the online version at <http://dx.doi.org/10.1016/j.bios.2013.09.003>.

References

- Allothman, Z.A., Bukhari, N., Wabaidur, S.M., Haider, S., 2010. *Sensors and Actuators B* 146, 314–320.
- Barreto, W.J., Barreto, S.R., Ando, R.A., Santos, P.S., DiMauro, E., Jorge, T., 2008. *Spectrochimica Acta A* 71, 1419–1424.
- Carrera, V., Sabater, E., Vilanova, E., Sogorb, M.A., 2007. *Journal of Chromatography B* 847, 88–94.
- Chen, J.L., Yan, X.P., Meng, K., Wang, S.F., 2011. *Analytical Chemistry* 83, 8787–8793.
- Chen, B., Li, F., Li, S., Weng, W., Guo, H., Guo, T., Zhang, X., Chen, Y., Huang, T., Hong, X., You, S., Lin, Y., Zeng, K., Chen, S., 2013. *Nanoscale* 5, 1967–1971.
- Dai, H., Xu, G., Gong, L., Yang, C., Lin, Y., Tong, Y., Chen, J., Chen, G., 2012. *Electrochimica Acta* 80, 362367.
- Deng, C., Chen, J., Wang, M., Xiao, C., Nie, Z., Yao, S., 2009. *Biosensors and Bioelectronics* 24, 2091–2094.
- El-Beqqali, A., Kussak, A., Abdel-Rehim, M., 2007. *Journal of Separation Science* 30, 421–424.
- Fernandes, S.C., Vieira, I.C., Peralta, R.A., Neves, A., 2010. *Electrochimica Acta* 55, 7152–7157.
- Frens, G., 1973. *Nature (London), Physical Sciences* 241, 20–22.
- Ge, B., Tan, Y., Xie, Q., Ma, M., Yao, S., 2009. *Sensors and Actuators B* 137, 547–554.
- Goldberg, L.L., 1972. *Pharmacological Reviews* 24, 1–29.
- Gonon, F., Buda, M., Cespuglio, R., Jouvert, M., Pajol, J., 1980. *Nature* 286, 902–904.
- Habibi, B., Jahanbakshi, M., Pournaghi-Azar, M.H., 2011. *Electrochimica Acta* 56 (7), 2888–2894.
- Hsu, M.S., Chen, Y.L., Lee, C.Y., Chiu, H.T., 2012. *ACS Applied Materials and Interfaces* 4, 5570–5575.
- Ji, X., Palui, G., Avellini, T., Na, H.B., Yi, C., Knappenberger, K.L., Mattoussi, H., 2012. *Journal of the American Chemical Society* 134, 6006–6017.
- Khattar, R., Mathur, P., 2013. *Inorganic Chemistry Communications* 31, 37–43.
- Kim, Y.R., Bong, S., Kang, Y.J., Yang, Y., Mahajan, R.K., Kim, J.S., Kim, H., 2010. *Biosensors and Bioelectronics* 25, 2366–2369.
- Laviron, E., 1979. *Journal of Electroanalytical Chemistry* 101, 19–28.
- Li, H., Li, C., Yan, Z.Y., Yang, J., Chen, H., 2010. *Journal of Neuroscience Methods* 189, 162–168.
- Liu, J.M., Lin, L.P., Wang, X.X., Lin, S.Q., Cai, W.L., Zhang, L.H., Zheng, Z.Y., 2012. *Analyst* 137, 2637–2642.
- Liu, M., Chen, Q., Lai, C., Zhang, Y., Deng, J., Li, H., Yao, S., 2013. *Biosensors and Bioelectronics* 48, 75–81.
- Luo, P., Li, C., Shi, G., 2012. *Physical Chemistry Chemical Physics* 14, 7360–7366.
- Muzzi, C., Bertocci, E., Terzuoli, L., Porcelli, B., Ciari, I., Pagani, R., Guerranti, R., 2008. *Biomedicine and Pharmacotherapy* 62, 253–258.
- Prasad, B.B., Jauhari, D., Tiwari, M.P., 2013. *Biosensors and Bioelectronics* 50, 19–27.
- Qian, T., Yu, C., Wu, S., Shen, J., 2013. *Biosensors and Bioelectronics* 50, 157–160.
- Raj, C.R., Ohsaka, T., 2001. *Journal of Electroanalytical Chemistry* 496, 44–49.
- Raj, C.R., Okajima, T., Ohsaka, T., 2003. *Journal of Electroanalytical Chemistry* 543, 127–133.
- Stoyanova, A., Ivanov, S., Tsakova, V., Bund, A., 2011. *Electrochimica Acta* 56, 3693–3699.
- Sulzer, D., 2011. *Neuron* 69, 628–649.
- Suzuki, I., Fukuda, M., Shirakawa, K., Jiko, H., Gotoh, M., 2013. *Biosensors and Bioelectronics* 49, 270–275.
- Thabano, J.R., Breadmore, M.C., Hutchinson, J.P., Johns, C., Haddad, P.R., 2009. *Journal of Chromatography A* 1216, 4933–4940.
- Wang, Y., Li, Y., Tang, L., Lu, J., Li, J., 2009b. *Electrochemistry Communications* 11, 889–892.
- Wightman, R.M., 2006. *Science Signaling* 311, 1570–1574.
- Xiao, C., Chu, X., Yang, Y., Li, X., Zhang, X., Chen, J., 2011. *Biosensors and Bioelectronics* 26, 2934–2939.
- Zhang, F., Li, Y., Gu, Y., Wang, Z., Wang, C., 2011. *Microchimica Acta* 173, 103–109.
- Zhang, M., Gong, K., Zhang, H., Mao, L., 2005. *Biosensors and Bioelectronics* 20, 1270–1276.